# Transepithelial migration of neutrophils into the lung requires TREM-1

Julia Klesney-Tait,[1] Kathy Keck,[1] Xiaopeng Li,[1] Susan Gilfillan,[2] Karel Otero,[2] Sankar Baruah,[1] David K. Meyerholz,[3] Steven M. Varga,[4] Cory J. Knudson,[4] Thomas O. Moninger,[5] Jessica Moreland,[6] Joseph Zabner,[1] and Marco Colonna[2]

[1]Department of Internal Medicine, University of Iowa Carver College of Medicine, Iowa City, Iowa, USA. [2]Department of Pathology, Washington University in St. Louis, St. Louis, Missouri, USA. [3]Department of Pathology, [4]Department of Microbiology, [5]Central Microscopy Research Facility, and [6]Department of Pediatrics, University of Iowa Carver College of Medicine, Iowa City, Iowa, USA.

**Acute respiratory infections are responsible for more than 4 million deaths each year. Neutrophils play an essential role in the innate immune response to lung infection. These cells have an armamentarium of pattern recognition molecules and antimicrobial agents that identify and eliminate pathogens. In the setting of infection, neutrophil triggering receptor expressed on myeloid cells 1 (TREM-1) amplifies inflammatory signaling. Here we demonstrate for the first time that TREM-1 also plays an important role in transepithelial migration of neutrophils into the airspace. We developed a TREM-1/3–deficient mouse model of pneumonia and found that absence of TREM-1/3 markedly increased mortality following *Pseudomonas aeruginosa* challenge. Unexpectedly, TREM-1/3 deficiency resulted in increased local and systemic cytokine production. TREM-1/3–deficient neutrophils demonstrated intact bacterial killing, phagocytosis, and chemotaxis; however, histologic examination of TREM-1/3–deficient lungs revealed decreased neutrophil infiltration of the airways. TREM-1/3–deficient neutrophils effectively migrated across primary endothelial cell monolayers but failed to migrate across primary airway epithelia grown at the air-liquid interface. These data define a new function for TREM-1 in neutrophil migration across airway epithelial cells and suggest that it amplifies inflammation through targeted neutrophil migration into the lung.**

## Introduction

Acute respiratory infections have been described as the forgotten pandemic, responsible for 4.5 million deaths annually. Effective neutrophil migration into the intrapulmonary airspace is essential for pathogen elimination in the lung. Neutrophils possess diverse tools, including ROS intermediates, antimicrobial peptides, neutrophil extracellular traps, and numerous pattern recognition receptors (PRRs), that facilitate the response to de novo infections (1, 2). Moreover, neutrophils participate in B cell maturation and differentiation, Th17 responses, dendritic cell maturation, natural killer cell responses, and IL-10 production, revealing a regulatory role for neutrophils (2). Like other cells of the innate immune system, neutrophils express several large genetically encoded receptor families that act to detect and eliminate pathogens. These families include the TLR family, C-type lectin receptors, and the triggering receptor expressed on myeloid cells (TREM) family (3–5).

TREM-1, which was initially discovered on human neutrophils and monocytes, has been studied in patients with pneumonia and sepsis (6, 7). Increased TREM-1 levels in bronchoalveolar lavage (BAL) fluid strongly correlate with ventilator-associated pneumonia, and systemic levels of TREM-1 in the serum serve as a marker of sepsis (8, 9). TREM-1 has been shown to amplify the inflammatory cascade in response to infection (10). Surface expression of TREM-1 is increased in response to LPS and other microbial products in vitro. Antibody-mediated crosslinking of TREM-1 induces modest cellular activation and proinflammatory cytokine secretion. Furthermore, when TREM-1 acts in concert with PRRs, there is a synergistic increase in inflammatory signaling (10–13). Such data suggest that TREM-1 functions as an amplifier of the immune response in the context of microbial infection.

During the process of pathogen recognition and elimination, excessive cytokine and chemokine release can lead to extensive tissue damage and even death (14, 15). Therapeutic agents designed to temper the deleterious consequences of host-pathogen interactions result in a survival benefit in some experimental models of endotoxemia. On the other hand, it is clear that some inflammation is necessary for bacterial killing in vivo. Accordingly, numerous clinical examples of impaired neutrophil function are linked to increased rates of infection and death, including chronic granulomatous disease (CGD), neutropenic fever, and lymphocyte adhesion deficiency. However, animal studies indicate that effective bacterial clearance can be achieved in the setting of decreased inflammation (16, 17). In the case of TREM-1, blockade of TREM-1 has been achieved by administering soluble forms of TREM-1, small molecule blocker (LP-17), or RNA silencing (10, 18, 19). All three of these interventions result in decreased systemic cytokine production and improved survival in mice. Taken together, these animal studies of TREM-1 blockade suggest that it may be possible to modulate the TREM-1 pathway to decrease inflammation without sacrificing bacterial control.

We hypothesized that TREM-1 deficiency would decrease inflammation and improve survival in a murine pneumonia model. Paradoxically, we found that TREM-1/3 deficiency resulted in a marked increase in mortality. Our data suggest that impaired neutrophil transepithelial migration is the mechanism underlying the failure to clear lung bacteria, resulting in increased mortality with TREM-1/3 deficiency. These findings identify a novel role for TREM-1 in neutrophil epithelial transmigration in addition to its established role in amplifying inflammatory signaling.

**Conflict of interest:** The authors have declared that no conflict of interests exists.
**Citation for this article:** *J Clin Invest.* 2013; 123(1):138–149. doi:10.1172/JCI64181.

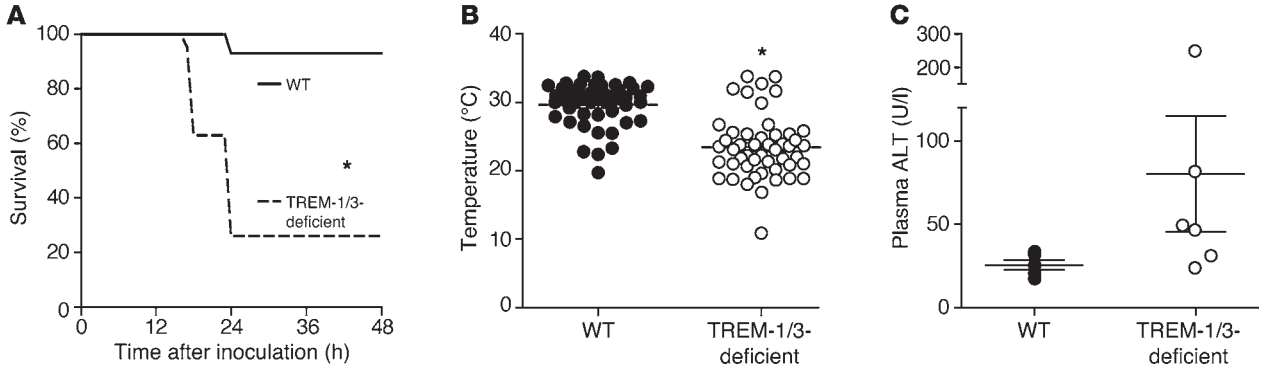


**Figure 1**
TREM-1/3 expression is essential for host survival following *P. aeruginosa* challenge. (**A**) Kaplan-Meier survival plot of TREM-1/3–deficient ($n$ = 35, 4 experiments) and WT mice ($n$ = 26, 4 independent experiments) following intratracheal challenge with *P. aeruginosa* (*$P$ = 0.0001). (**B**) Body temperature was measured 14 hours after infection with *P. aeruginosa* (*$P$ = 0.0001) ($n$ = 95 mice, 9 experiments). (**C**) As a marker of liver damage, ALT levels were measured 14 hours after intratracheal challenge with *P. aeruginosa* ($n$ = 11).

## Results

*Generation of TREM-1–deficient mice*. The goal of these studies was to elucidate the role of TREM-1 in pneumonia using a mouse model of TREM-1 deficiency. In mice, the *Trem1* gene is adjacent to a highly homologous gene, *Trem3*, which likely arose from a duplication event. The two receptors have similar cellular distribution and associate with DAP12. Further suggesting that these two proteins have redundant functions in the mouse, functional studies in our laboratory and others show that both molecules are amplifiers of inflammatory signaling (20). In contrast, *Trem3* is a pseudogene in humans, and therefore no functional overlap exists. Thus, to model the effect of blocking TREM-1 in humans, we generated a TREM-1/3–deficient mouse. To abrogate expression of functional TREM-1 and TREM-3 proteins, we made a targeting construct in which an 8.8-kb fragment containing most of exon 3 and exon 4 of *Trem1* as well as exon 1 of *Trem3* was replaced with a MC1neopA gene flanked by loxP sites (Supplemental Figure 1; supplemental material available online with this article; doi:10.1172/JCI64181DS1). This effectively deleted the transmembrane region of TREM-1 in addition to the start site and first domain of TREM-3. Chimeras generated from a correctly targeted clone were bred to transgenic mice expressing Cre under the CMV promoter on a C57BL/6 background to delete the MC1neopA gene. Homozygote TREM-1/3–deficient mice failed to express TREM-1 and TREM-3 proteins (Supplemental Figure 2). Inheritance of this mutation followed expected Mendelian distribution, with 25% homozygotes, 21% WT, and 54% heterozygotes assayed ($n$ = 229). Flow cytometric analysis using lineage markers revealed no significant differences in the percentages of circulating leukocyte populations as a result of *Trem1* and *Trem3* deletion (Supplemental Figure 3).

*TREM-1/3 is essential for host survival following pulmonary challenge with P. aeruginosa*. To examine the role of TREM-1 in survival in response to pneumonia, we challenged TREM-1/3–deficient mice, WT littermate controls, or WT C57BL/6 mice intratracheally with *P. aeruginosa*. Survival analysis performed using Gehan-Breslow-Wilcoxon statistical tests showed a significant increase in mortality in TREM-1/3–deficient mice as compared with WT mice, with $\chi^2$ = 18.75 and $P$ < 0.0001 (Figure 1A). Additional clinical indicators of sepsis including body temperature and evidence of end-organ damage were monitored. TREM-1/3–deficient animals were hypothermic (Figure 1B, $P$ = 0.0001), consistent with the development of systemic disease. TREM-1/3–deficient animals also showed evidence of end-organ damage in the form of transaminitis as measured by serum alanine aminotransferase (ALT) levels, whereas WT animals had no elevation (Figure 1C). These data indicate that TREM-1/3 expression is essential for host survival following pulmonary chal-

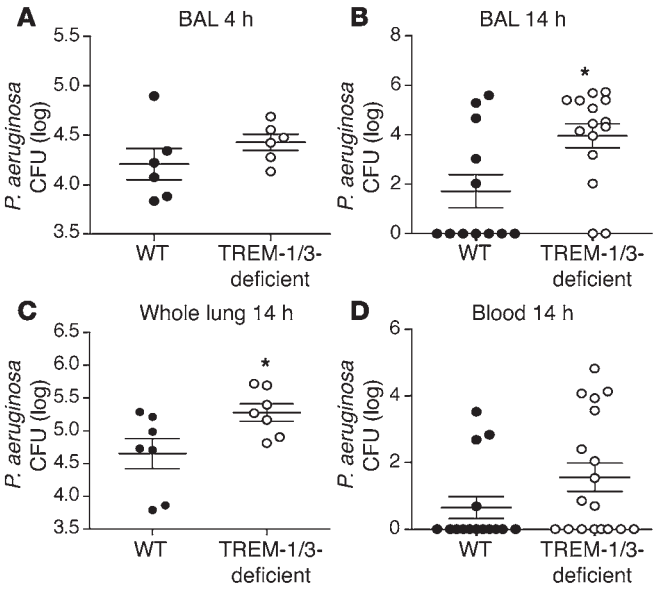


**Figure 2**
TREM-1/3–deficient mice fail to eradicate *P. aeruginosa* following pulmonary challenge. (**A**) CFU of *P. aeruginosa* in BAL fluid at 4 hours after infection in WT and TREM-1/3–deficient mice ($n$ = 12, 1 experiment). (**B**) CFU of *P. aeruginosa* in BAL from WT and TREM-1/3–deficient mice 14 hours after infection (*$P$ = 0.011) ($n$ = 27, 2 independent experiments). (**C**) CFU of *P. aeruginosa* recovered in whole lung homogenates from WT and TREM-1/3–deficient mice 14 hours after infection (*$P$ = 0.036) ($n$ = 14, 1 experiment). (**D**) CFU of *P. aeruginosa* recovered from cardiac puncture 14 hours after inoculation in TREM-1/3–deficient and WT mice ($n$ = 27, 2 independent experiments).

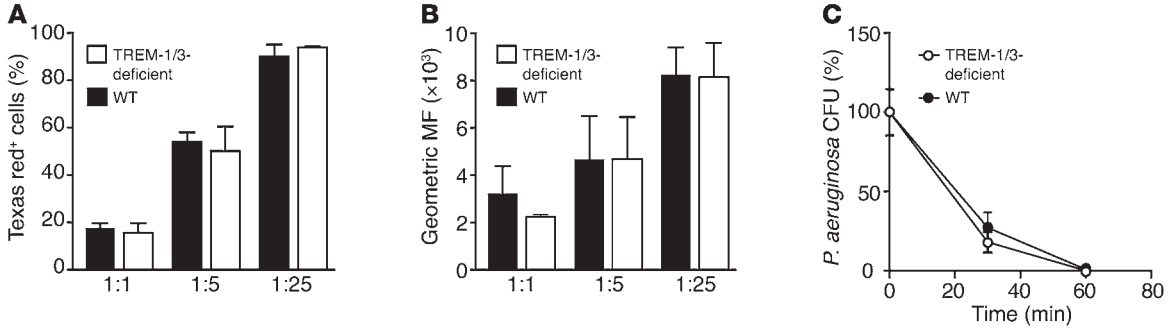


**Figure 3**
TREM-1/3–deficient neutrophils effectively kill *P. aeruginosa*. (**A**) TREM-1/3–deficient and WT neutrophil phagocytosis of Texas red–labeled zymosan particles was quantitated as the percentage of cells ingesting particles (2 independent experiments; pooled neutrophils from 2–3 mice per group). (**B**) The relative number of Texas red–labeled particles ingested per neutrophil was also quantified using the geometric MF of Texas red–positive TREM-1/3–deficient and WT neutrophils. (**C**) The ability of TREM-1/3–deficient and WT bone marrow neutrophils to kill *P. aeruginosa* was measured (3 independent experiments; pooled neutrophils from 2–3 mice per group).

lenge with *P. aeruginosa*. Challenge with heat-killed *P. aeruginosa* resulted in no mortality in WT or TREM-1/3–deficient mice ($n = 4$ in each group, data not shown), suggesting that the difference in survival observed in the TREM-1/3–deficient mice was due to a decrease in the ability to control active infection and not increased inflammation in the setting of endotoxin challenge.

*TREM-1/3–deficient animals fail to eradicate P. aeruginosa*. To assess bacterial clearance, we performed bacterial sampling of BAL fluid using whole lung lavage on anesthetized animals at either 4 or 14 hours after infection. At 4 hours after infection, both TREM-1/3–deficient and WT BAL fluid (Figure 2A) showed growth of *P. aeruginosa*. However, at 14 hours after infection, *P. aeruginosa* CFU were higher in the lungs of TREM-1/3–deficient animals (Figure 2B, $P = 0.011$). In addition, *P. aeruginosa* CFU were also significantly higher in cultures obtained from whole lung suspensions generated 14 hours after infection in TREM-1/3–deficient as compared with WT mice (Figure 2C, $P = 0.036$). Next, blood was obtained by cardiac puncture 14 hours after infection to assess systemic bacteremia (Figure 2D). TREM-1/3–deficient animals had a higher incidence of bacteremia (53% TREM-1/3–deficient vs. 27% WT). Thus, TREM-1/3–deficient mice fail to eradicate *P. aeruginosa* infection locally, resulting in systemic dissemination of bacteria and death.

*TREM-1/3–deficient neutrophils kill P. aeruginosa effectively in vitro*. To assess whether impaired neutrophil function was the mechanism for poor local and systemic control of *P. aeruginosa* in the TREM-1/3–deficient animals, we measured phagocytosis and in vitro neutrophil killing of *P. aeruginosa*. First, phagocytosis was measured using Texas red–zymosan. Neutrophils were isolated from TREM-1/3–deficient and WT bone marrow (pooled 3–5 per group). There were no significant differences in the percentage of neutrophils that ingested particles (Figure 3A) or in the number of particles phagocytized per neutrophil as determined by the geometric mean of Ly6G-positive cells (Figure 3B). To distinguish between intracellular and extracellular particles, we performed

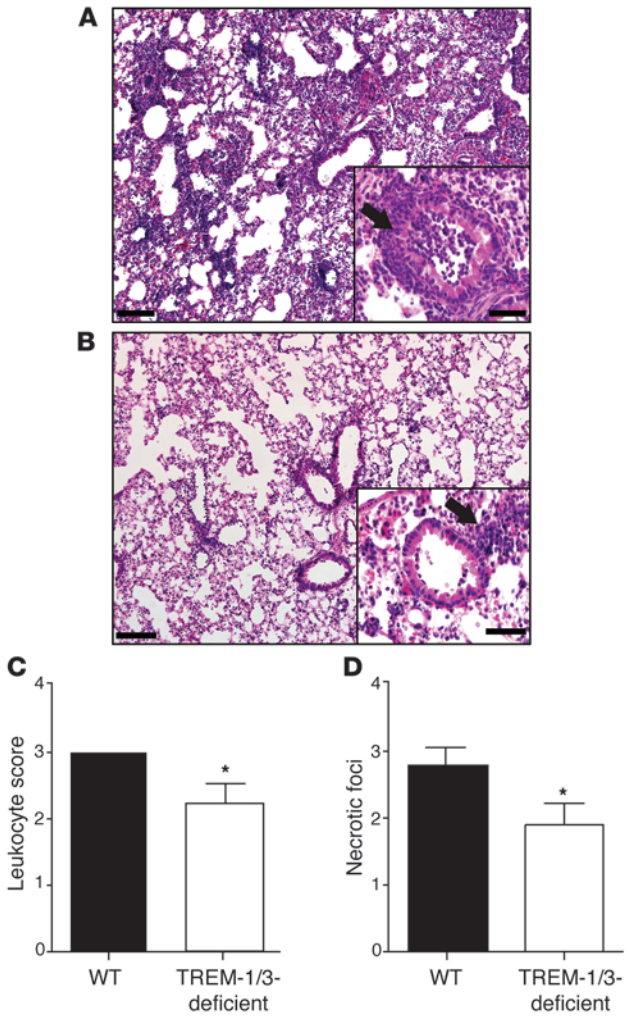


**Figure 4**
TREM-1/3–deficient mice have decreased histologic evidence of pneumonia following *P. aeruginosa* challenge. (**A** and **B**) Representative H&E-stained lungs from (**A**) WT or (**B**) TREM-1/3–deficient mice 14 hours after infection with *P. aeruginosa*. Original magnification, ×10; inset, ×60. Arrows indicate areas of necropurulent foci. ×10 scale bar: 140 μm; ×60 scale bar: 50 μm. (**C**) Leukocyte infiltration score in lungs from WT and TREM-1/3–deficient mice 14 hours after infection ($n = 10$ mice, $^*P = 0.016$). (**D**) Necrotic foci score in lungs of WT and TREM-1/3–deficient mice 14 hours after infection ($n = 10$ mice, $^*P = 0.05$). Error bars indicate SEM.

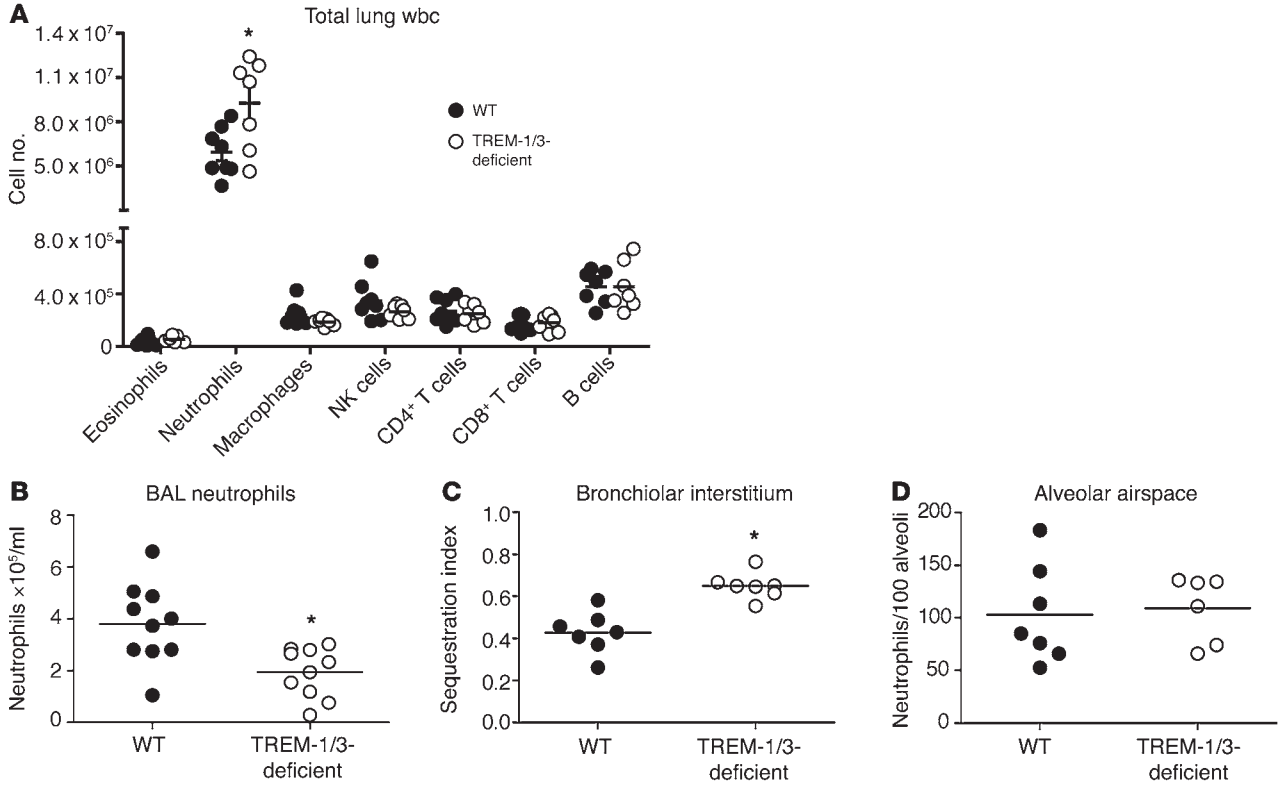


**Figure 5**
Quantification of neutrophils in lung compartments following *P. aeruginosa* challenge. (**A**) Quantification of total wbc populations in single-cell suspensions from lungs of WT and TREM-1/3–deficient mice 14 hours after infection ($n = 15$, $^*P = 0.001$). (**B**) Quantification of neutrophils present in BAL of WT and TREM-1/3–deficient mice 14 hours after infection ($n = 20$, $^*P = 0.004$, 2 independent experiments) (**C**) Morphometric analysis of the neutrophils in the interstitium of terminal bronchioles from the lungs of WT and TREM-1/3–deficient mice ($n = 14$, $^*P = 0.001$). (**D**) Stereotactic analysis of alveolar neutrophils from the lungs of WT and TREM-1/3–deficient animals ($n = 14$, $P = 0.79$). Error bars indicate SEM.

fluorescence quenching with trypan blue (21). No significant difference in quenching was detected between WT and TREM-1/3–deficient neutrophils (Supplemental Figure 4). Next, to examine the capacity of murine neutrophils to kill *P. aeruginosa,* we isolated neutrophils and co-incubated them with bacteria (22). At 30 minutes, more than 90% of the bacteria were ingested. Non-ingested bacteria were killed with gentamicin, as previously described (23). Intracellular bacterial killing was assessed at 30, 60, and 90 minutes after exposure to gentamicin. There was no significant difference in the ability of TREM-1/3–deficient and WT neutrophils to kill *P. aeruginosa* (Figure 3C). Finally, to determine how TREM-1/3 deficiency affects neutrophil ROS production, we isolated neutrophils from WT and TREM-1/3–deficient animals and stimulated them with opsonized zymosan and PMA. In the presence of no agonist, neither set of neutrophils produced ROS (Supplemental Figure 5), indicating that the neutrophils had not been activated in the isolation process. However, TREM-1/3–deficient neutrophils had a 50% reduction in ROS production in response to opsonized zymosan as compared with WT neutrophils (Supplemental Figure 5), whereas ROS production in response to PMA was intact (Supplemental Figure 5). It is well established that neutrophils eliminate *P. aeruginosa* through a number of $O_2$-independent pathways, including bactericidal/permeability-increasing protein (BPI), proteases, lipases, and defensins (24). In fact, neutrophils isolated from patients with CGD (an inherited defect in NADPH oxidase resulting in severely impaired ROS production) effectively kill *P. aeruginosa*, indicating that ROS production is not required in order to effectively kill this organism (24). Therefore, given the in vitro killing data, the striking in vivo phenotype in the TREM-1/3–deficient mice is likely not due to an intrinsic neutrophil killing defect.

*Lungs from TREM-1/3–deficient mice have decreased histologic evidence of pneumonia.* Histologic examination of lungs harvested from live mice at 14 hours after infection showed an unexpected difference. Lung tissue from 5 TREM-1/3–deficient animals and 5 WT animals was analyzed by a veterinary pathologist unaware of sample identities. The degree of inflammation was quantified as described in the Methods. TREM-1/3–deficient animals had less evidence of inflammation/pneumonia as compared with WT animals (Figure 4, A and B). Moreover, TREM-1/3–deficient animals had reduced leukocyte infiltration by morphometry ($P = 0.016$) and fewer necropurulent foci ($P = 0.05$) present in the lungs as compared with WT animals (Figure 4, C and D, respectively). Taken together, these data indicate that, despite increased bacterial load and higher mortality, TREM-1/3–deficient animals have impaired pulmonary inflammation in response to *P. aeruginosa* challenge.

*TREM-1/3–deficient animals have decreased neutrophils in the airway.* To assess leukocyte migration into the lung, first we asked whether there was a defect in wbc translocation into the lung. Single-cell suspension of lungs from WT and TREM-1/3–deficient animals were prepared to quantitate total lung wbc. TREM-1/3–deficient

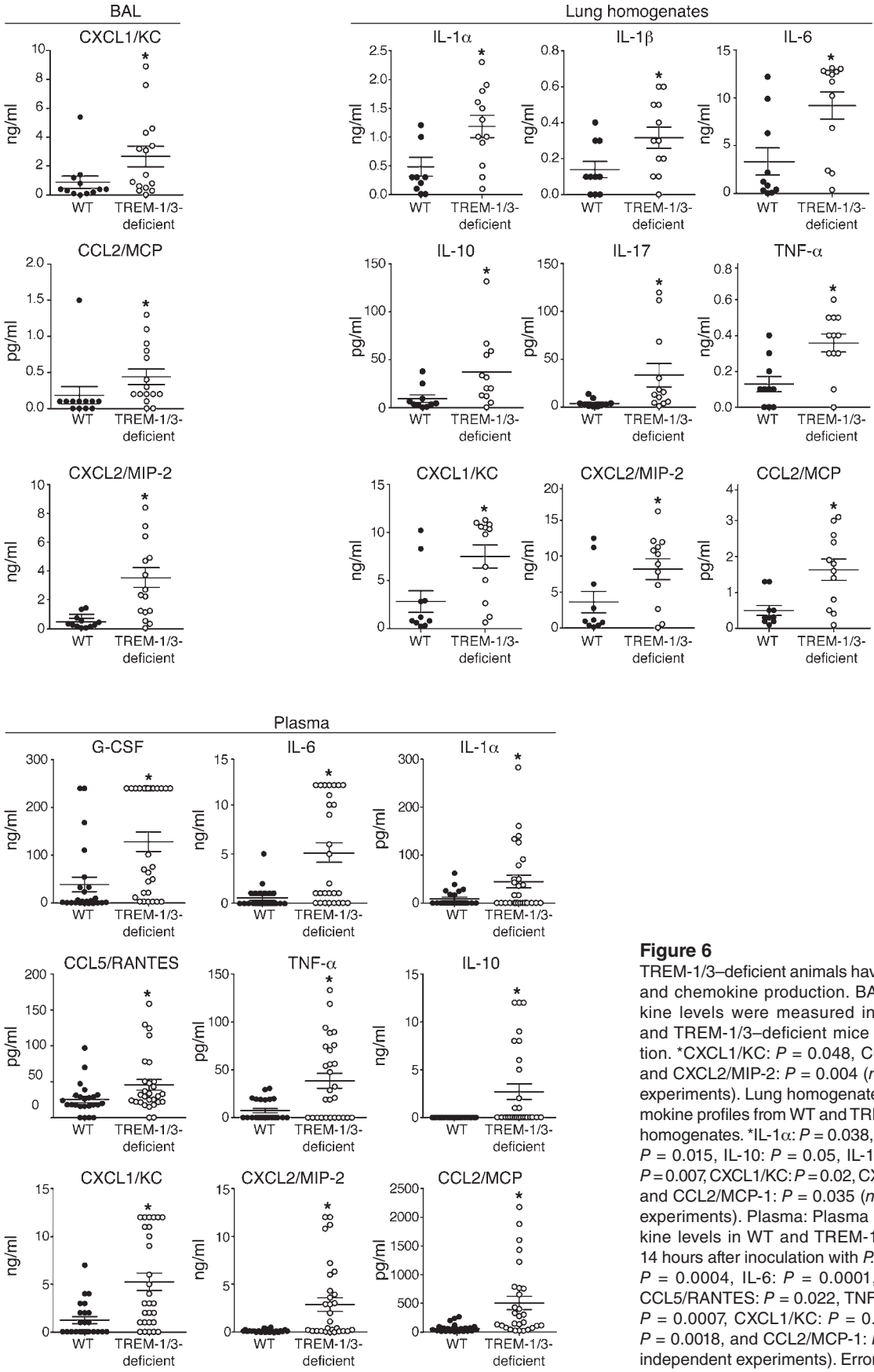


**Figure 6**

TREM-1/3–deficient animals have intact local cytokine and chemokine production. BAL: Indicated chemokine levels were measured in BAL fluid from WT and TREM-1/3–deficient mice 14 hours after infection. *CXCL1/KC: $P = 0.048$, CCL2/MCP: $P = 0.017$, and CXCL2/MIP-2: $P = 0.004$ ($n = 27$, 3 independent experiments). Lung homogenates: Cytokine and chemokine profiles from WT and TREM-1/3–deficient lung homogenates. *IL-1α: $P = 0.038$, IL-1β: $P = 0.038$, IL-6: $P = 0.015$, IL-10: $P = 0.05$, IL-17: $P = 0.022$, TNF-α: $P = 0.007$, CXCL1/KC: $P = 0.02$, CXCL2/MIP-2: $P = 0.012$, and CCL2/MCP-1: $P = 0.035$ ($n = 22$, 2 independent experiments). Plasma: Plasma cytokine and chemokine levels in WT and TREM-1/3–deficient mice at 14 hours after inoculation with *P. aeruginosa*. *G-CSF: $P = 0.0004$, IL-6: $P = 0.0001$, IL-1α: $P = 0.0448$, CCL5/RANTES: $P = 0.022$, TNF-α: $P = 0.0072$, IL-10: $P = 0.0007$, CXCL1/KC: $P = 0.0011$, CXCL2/MIP-2: $P = 0.0018$, and CCL2/MCP-1: $P = 0.0002$ ($n = 28$, 3 independent experiments). Error bars indicate SEM.

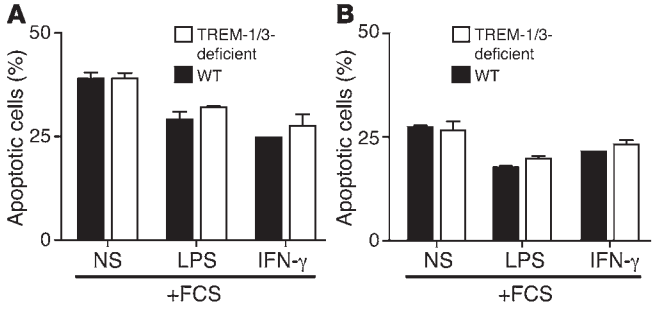


**Figure 7**
TREM-1/3–deficient neutrophils undergo cell death at rates similar to those of WT neutrophils. (**A** and **B**) WT and TREM-1/3–deficient neutrophil cell death was measured in vitro at rest (NS, not stimulated) and with stimulation with LPS or IFN-γ in the absence (**A**) or presence (**B**) of FCS. Representative data, 3 independent experiments. Error bars indicate SEM.

animals had similar numbers of eosinophils, macrophages, NK cells, $CD4^+$ T cells, $CD8^+$ T cells, and B cells (Figure 5A, $n = 15$). Unexpectedly, the number of total lung neutrophils was significantly higher in TREM-1/3–deficient animals (Figure 5A, $P = 0.001$). Therefore, despite having more total lung neutrophils, TREM-1/3–deficient mice failed to develop pneumonia with consolidation and were unable to clear *P. aeruginosa* lung infection, resulting in a marked increase in mortality.

Next, we determined using BAL whether TREM-1/3–deficient mice have defective neutrophil translocation into the airspace. More than 96% of all cells from the BAL fluid of both groups were Ly6G positive and CD115 negative (data not shown), consistent with murine neutrophil identity. TREM-1/3–deficient mice had a 50% reduction in the number of airway neutrophils (Figure 5B, $P = 0.004$), suggesting impaired migration of neutrophils into the airspace. We then used a stereological approach to further localize neutrophils in the compartments of the lung by specifically examining the interstitium, the airway lumen (terminal bronchioles), and the alveolar space. To assess the location of neutrophils in the distal airways, we identified terminal bronchioles and a sequestration index was calculated to assess the relative number of neutrophils in the interstitium versus the distal airway lumen. Terminal bronchioles from TREM-1/3–deficient mice had a higher sequestration index as compared with WT mice (Figure 5C, $n = 13$, $P = 0.001$), indicating that a higher proportion of neutrophils was present in the interstitial space as compared with the lumen and suggesting a neutrophil migratory block into the bronchiolar airway. There was no detectable difference in the number of neutrophils in the alveolar compartment in WT and TREM-1/3–deficient mice (Figure 5D). The features of consolidation and alveolar collapse were at times confounding issues, and it remains unclear whether a migratory block at the alveolar level exists in TREM-1/3–deficient mice. Taken together, the histologic data and BAL data indicate that, with TREM-1/3 deficiency, there is a defect in neutrophil migration into the airspace.

*TREM-1/3–deficient mice have increased cytokine production both locally and systemically following P. aeruginosa challenge.* Because TREM-1 acts synergistically with TLR and other PRRs to augment proinflammatory cytokine production, we hypothesized that a blunted cytokine response to infection with *P. aeruginosa* would be responsible for decreased airway neutrophils in TREM-1/3–deficient animals. Cytokines were sampled in the plasma, BAL fluid, and total lung homogenates. To avoid survivor bias, all samples were collected at 14 hours following infection, when all animals in both groups were alive. First, to ascertain whether decreased neutrophil migration was the result of a deficiency in local chemokine production, we obtained BAL fluid from infected mice. CXCL1/KC, CXCL2/MIP-2, and CCL2/MCP were elevated in TREM-1/3–deficient as compared with WT mice, consistent with sufficient local production of chemoattractants (Figure 6, BAL: $P = 0.048$, $P = 0.017$, and $P = 0.004$, respectively). In separate experiments, total tissue cytokine levels were measured in lungs harvested from anesthetized TREM-1/3–deficient and WT mice after perfusion with PBS from the right ventricle to remove intravascular blood (Figure 6, Lung homogenates). TREM-1/3–deficient mice had higher levels of IL-1α ($P = 0.038$), IL-1β ($P = 0.038$), IL-6 ($P = 0.015$), IL-10 ($P = 0.05$), IL-17 ($P = 0.022$), and TNF-α ($P = 0.007$) and chemokines CXCL1/KC ($P = 0.02$), CXCL2/MIP-2 ($P = 0.012$), and CCL2/MCP-1 ($P = 0.035$). Based on these results and those shown in Figures 4 and 5, we conclude that despite elevated local cytokines and chemokines, TREM-1/3–deficient animals have ineffective accumulation of neutrophils in the airway lumen.

Additionally, systemic cytokine levels were measured (Figure 6). The TREM-1/3–deficient mice had statistically significant increases in the proinflammatory cytokines G-CSF, IL-6, IL-1α, CCL5/RANTES, TNF-α, IL-12p40 ($P = 0.004$, data not shown), and IL12-p70 ($P = 0.020$, data not shown); increased levels of chemoattractants CXCL1 /KC, CCL2/MCP-1, CXCL2/MIP-2; and increased anti-inflammatory cytokine IL-10. These data indicate that the cytokine production was not impaired in the setting of infection despite the loss of the TREM-1/3 amplifying pathway. Moreover, these data indicate that impaired cytokine production was not responsible for the decrease in neutrophils in the airway lumen of TREM-1/3–deficient animals.

*TREM-1/3–deficient neutrophils have normal cell death.* To investigate whether the diminished number of neutrophils in the airways of TREM-1/3–deficient animals was due to increased cell death, we isolated neutrophils from TREM-1/3–deficient and WT animals and determined cell death by propidium iodide uptake as previously described (25). We observed no significant difference in the percentage of neutrophils undergoing cell death spontaneously or

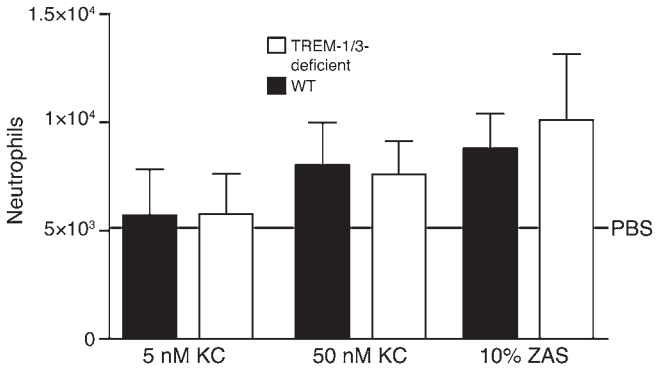


**Figure 8**
Deficiency of TREM-1/3 does not abrogate in vitro neutrophil chemotaxis in response to chemokines. WT and TREM-1/3–deficient neutrophil chemotaxis was measured in response to chemoattractants KC (5 nM, 50 nM) and 10% ZAS. The line labeled PBS indicates the number of chemotactic neutrophils relative to the PBS control. Representative data; $n = 2$–3 mice pooled per group; 3 independent experiments. Error bars indicate SEM.

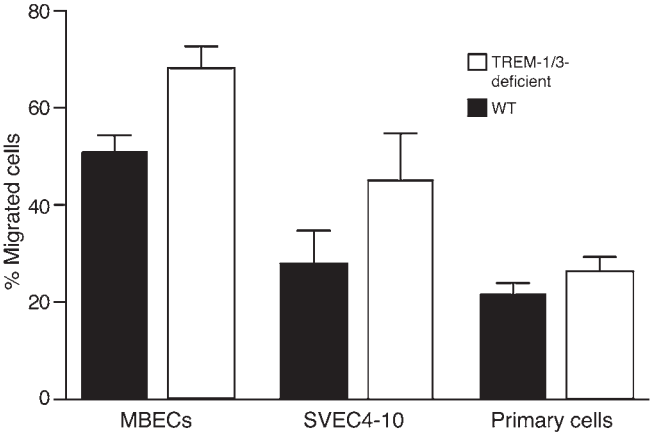


**Figure 9**
TREM-1/3–deficient neutrophils have intact transendothelial migration. The ability of WT and TREM-1/3–deficient neutrophils to migrate across murine endothelial cell monolayers (SVEC4-10 cells and MBECs) and primary murine lung endothelial cell monolayers was measured in response to stimulation with 10% ZAS. Representative data, $n = 2–3$ mice pooled per group, 3 independent experiments. Error bars indicate SEM.

in response to LPS or IFN-γ in the absence or presence of serum (Figure 7, A and B, respectively). Therefore, impaired neutrophil survival is likely not the mechanism of decreased neutrophil accumulation in the airways of TREM-1/3–deficient animals.

*In vitro chemokine-induced migration is intact in TREM-1/3–deficient neutrophils.* Next, we examined neutrophil migration using the TX migration plate (see Methods) to determine whether the defect in neutrophil accumulation in the airway of TREM-1/3–deficient mice was the result of an intrinsic defect in the ability of TREM-1/3–deficient neutrophils to respond to chemoattractants. Neutrophils were placed in the upper compartment of chambers separated from the lower compartment by a filter with 3-μm pores. Zymosan-activated serum (ZAS) or CXCL-1/KC was added to the lower chamber as a chemoattractant. There was no significant difference in migration between WT and TREM-1/3–deficient cells (Figure 8), indicating that deficiency in TREM-1/3 does not alter the migratory response to chemoattractants.

*TREM-1/3–deficient neutrophils have intact transendothelial migration.* The first step in neutrophil migration into infected airways is neutrophil migration from the vasculature across the pulmonary capillary endothelial cell monolayer. We hypothesized that TREM-1/3 may interact with endothelial cell receptors to facilitate neutrophil migration across the endothelial cell barrier. Therefore, we examined whether TREM-1/3–deficient neutrophils had an impaired ability to cross endothelial cell monolayers in vitro. Murine endothelial cells lines (SVEC4-10 and murine brain endothelial cells [MBECs]) were seeded on 3-μm-pore-size Transwell filters and grown to confluence. Freshly isolated bone marrow–derived neutrophils were loaded on the apical side of the endothelial monolayers, and ZAS (10%), a neutrophil chemoattractant, was added to the opposite side. There was no defect in the ability of TREM-1/3–deficient neutrophils to migrate across murine endothelial cell monolayers as compared with WT neutrophils (Figure 9). In addition, we repeated the experiments using primary murine endothelial cells cultured as previously described (26). Consistent with the cell line data, we observed similar migration of TREM-1/3–deficient and WT neutrophils across primary murine endothelial cell monolayers (Figure 9). These data suggest that impaired transendothelial migration is not the mechanism of decreased neutrophils in the airway of TREM-1/3–deficient mice following *P. aeruginosa* challenge.

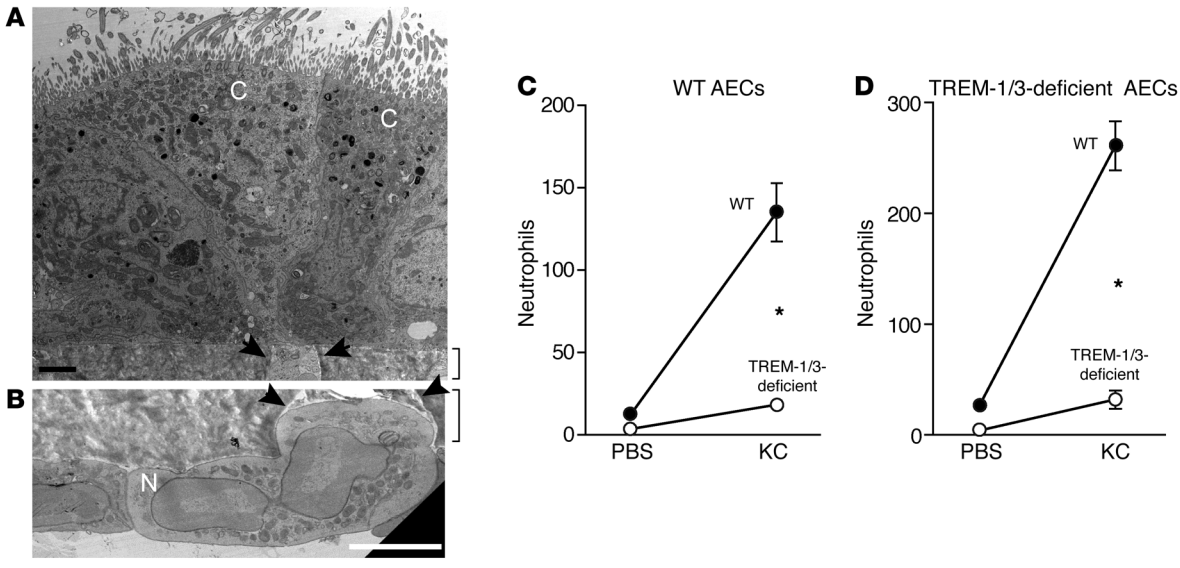


**Figure 10**
TREM-1/3 are required for neutrophil migration across AEC monolayers. (**A**) TEM image the air-interface cultured primary murine airway epithelia, including 2 ciliated cells (C). (**B**) TEM image of a neutrophil (N) attached to the underside of the Transwell filter prior to migration through a pore. Brackets indicate the filter; arrowheads indicate each side of a pore. Scale bars: 2 μm. (**C**) Migration of WT and TREM-1/3–deficient neutrophils across WT AECs in response to KC or PBS control was measured. *$P = 0.02$ vs. WT neutrophil migration to KC. (**D**) WT and TREM-1/3–deficient neutrophil migration across TREM-1/3–deficient AECs was measured as in **C**. *$P = 0.02$ vs. WT neutrophil migration to KC. Representative data; $n = 3$ mice pooled per group; 2 independent experiments. Error bars indicate SEM.

*TREM-1/3–deficient neutrophils have a defect in transepithelial migration.* In vivo, once neutrophils migrate from the capillaries, they must cross a pseudo-stratified epithelium to enter the luminal side of the airway. Airway epithelial cells (AECs) are polarized, and neutrophil transepithelial migration occurs from the basolateral side of AEC to the apical side of AEC into the airway lumen. Therefore, the ability of TREM-1/3–deficient neutrophils to migrate across primary polarized AECs was examined. While TREM-1 and TREM-3 are not known to be expressed on AECs, to eliminate an AEC defect in TREM-1/3–deficient mice as the source of impaired migration, we cultured both WT and TREM-1/3–deficient primary murine tracheal AECs on Transwells using previously described methods (27). The differentiated AECs from WT and TREM-1/3–deficient mice established transepithelial resistance greater than 500 $\Omega \cdot cm^2$, indicating the presence of tight junctions. Transmission electron micrograph (TEM) images of the murine airway epithelial monolayers demonstrate ciliate cell features (Figure 10A). Figure 10B depicts a neutrophil attached to underside of the Transwell filter before migration. Freshly isolated bone marrow–derived neutrophils (pooled from 3 mice per group) were loaded on the basolateral side of AECs by inversion of the Transwells. CXCL1/KC was added as a chemoattractant to the culture medium on the apical side of the epithelium. Migration of WT neutrophils was similar across WT and TREM-1/3–deficient AECs ($P = 0.19$). By contrast, TREM-1/3–deficient neutrophils demonstrated a significant migratory defect in response to CXCL1/KC across both WT (Figure 10C) and TREM-1/3–deficient AECs (Figure 10D). Treatment of WT neutrophils with a TREM-1 polyclonal antibody but not a TREM-3 monoclonal antibody decreased migration across WT AECs (data not shown). Together, these data suggest that TREM-1 functions in neutrophil migration across AECs and that impaired neutrophil migration is the defect responsible for the susceptibility of TREM-1/3–deficient mice to *P. aeruginosa* pneumonia.

## Discussion

More than 2 million people die of pneumonia annually worldwide, most of them children under the age of 5 (28). These deaths occur at extremes of the immune response: too much inflammation and its associated lung injury can cause death, and insufficient inflammation and failure to clear infection can lead to the same result. Here, we identify TREM-1 as a novel receptor required for neutrophil transepithelial migration into the airway lumen. Our data suggest a mechanism by which impaired migration results in decreased neutrophil recruitment and ineffective bacterial clearance. Subsequently, the TREM-1–deficient animals die due to excessive cytokine release and bacterial dissemination. Thus, potential therapeutic agents to treat pneumonia, such as TREM-1 inhibitors, must achieve a balance between pathogen control and host tissue damage.

The neutrophil response is titrated not only through regulated cytokine and antimicrobial product release but also via controlled migration into the lung. Indeed, recent studies using intravital microscopy document the complexity of neutrophil migration (29, 30). These cells can immediately cross an endothelial cell barrier, pause and decide not to cross, or even cross and then reverse course to return to the vessel lumen, suggesting that the neutrophil is capable of integrating complex environmental signals (30). Determining how neutrophil migration is influenced by these disparate signals is critical for understanding the pathogenesis of pneumonia, acute respiratory distress syndrome, and other inflammatory diseases of the lung. The role of TREM-1 in cytokine augmentation has been well described, and our data demonstrate that TREM-1 is also involved in the process of neutrophil transepithelial migration.

Neutrophil migration into infected tissues has been studied extensively (31, 32). In the systemic circulation, the initial site of emigration is the postcapillary venule. Here, the neutrophil undergoes capture and rolling on the endothelial surface, and selectin family members play a critical role (33–35). Once firm adhesion has been established, transendothelial migration occurs under these laminar flow conditions. In contrast, neutrophil migration in the lung occurs in the pulmonary capillaries. Here a complex web of anastomosing capillaries requires the neutrophil to deform in order to pass through the vessels (36–38). Spatial constraints in the capillary most likely supplant the need for rolling and capture in the pulmonary circulation (39), thus providing an explanation for the fundamental difference in neutrophil migration in the lung compared with the systemic circulation. On the pulmonary endothelium, firm adhesion is primarily mediated by the interaction between the $\beta_2$ integrins CD18/CD11a (also LFA-1 or $\alpha L\beta 2$) and CD18/CD11b (also Mac-1 or $\alpha M\beta 2$) expressed on the neutrophils and ICAM-1 (also CD54), ICAM-2, and ICAM-3 expressed on the endothelial cell surface (40–42). Both homotypic and heterotypic interactions between PECAM-1 (CD31), CD177, $\beta_2$ integrins, ICAM-1, and junctional adhesion molecule (JAM) family members facilitate transendothelial migration (43–46). Because we observed decreased neutrophil accumulation in the lung airspace in TREM-1/3–deficient mice, we initially hypothesized that TREM-1/3 deficiency would cause defective transendothelial migration. However, TREM-1/3–deficient neutrophils migrated effectively across both murine endothelial cell lines and primary murine endothelial cells, likely via these previously described pathways, suggesting that TREM-1/3 is not required for transendothelial migration.

Compared with transendothelial migration, the molecular details of transepithelial migration are less well understood, including the extent to which neutrophils infiltrate the lung at the level of the large airway, the small airway, and/or the alveolar epithelia. Moreover, transepithelial migration is a dynamic process, and neutrophil passage through the alveolar interstitium is difficult to quantitate macroscopically. Our in vitro data using large airway epithelia grown at the air-liquid interface support a defect in neutrophil transepithelial migration. However, a limitation of our study is that we are unable to culture alveolar epithelia at the air-liquid interface for in vitro testing. In our model of TREM-1/3 deficiency, we detected differential compartmentalization of neutrophils in the interstitial space at the level of the small airway in vivo, consistent with a defect in transepithelial migration.

The integrity of the airway epithelium is achieved via tight junctions and adherens junction protein interactions. Paracellular migration is presumably achieved through alterations in tight junction protein interactions. Neutrophil adherence to the pulmonary epithelial cell layer is mediated by $\beta_2$ integrins, in particular CD18/CD11b and ICAM, though CD11a and CD11c may play some role (47–55). The role of JAMs in intestinal transepithelial migration has also been studied. For example, JAM C but not JAM A has been implicated in intestinal neutrophil transepithelial migration, with studies demonstrating that JAM C antibodies decrease the rate of neutrophil transepithelial migration but do not block migration (56). Recently a role for junctional adhesion molecule–like protein (JAML), which is expressed on neutrophils,

was described in intestinal transepithelial migration (57). JAML binds to epithelial cell via the coxsackie and adenovirus receptor (CAR), and soluble forms of either of these molecules impede neutrophil transepithelial migration across cultured intestinal epithelium. CD47, which is expressed on both epithelial cells and neutrophils, is also required for intestinal neutrophil transepithelial migration, though the mechanism is still being characterized and no studies have been conducted in the lung epithelium (58). To date there is no evidence for an interaction between TREM-1 and any of these adhesion molecules, suggesting that alternative mechanisms exist by which TREM-1 mediates neutrophil adhesion and migration across epithelial cells.

In this study, we demonstrate that loss of TREM-1/3 expression results in impaired neutrophil transepithelial migration in a murine pneumonia model. Gibot and colleagues examined the role of TREM-1 in bacterial pneumonia using a different approach (17). Their study involved instillation of a TREM-1–blocking peptide, LP-17, into the rat trachea following pneumonia challenge. Interestingly, this resulted in decreased lung inflammation and improved survival. Blockade of TREM-1–mediated amplification of cytokine production was thought to be the mechanism behind improved survival. However, our data suggest that LP-17 may play a role in blocking neutrophil migration. We propose that a partial blockade of neutrophil migration into the airways may allow a sufficient quantity of neutrophils to clear the infection but prevent extensive lung injury by attenuating transepithelial migration.

In summary, our results implicate TREM-1 as a novel player in neutrophil pulmonary transepithelial migration. We hypothesize that the TREM-1 interaction with the pulmonary epithelium provides a second novel regulatory pathway in vivo for TREM-1 to amplify inflammation through targeted migration into lung. In the absence of TREM-1, in vivo neutrophil migration to the airway lumen is impaired. This leads to ineffective bacterial killing and increased mortality. Further study of the role of TREM-1/3 molecules in transepithelial migration may identify therapeutic targets to modulate neutrophil influx, thereby altering the local inflammatory response not through classic cytokine signaling but through controlled migratory access.

## Methods

*Generation of TREM-1/3–deficient mice*. To abrogate expression of functional TREM-1 and TREM-3 proteins, we made a targeting construct in which an 8.8-kb fragment containing most of exon 3 and exon 4 of TREM-1 as well as exon 1 of TREM-3 was replaced with an MC1neopA gene flanked by loxP sites (Supplemental Figure 1). This effectively deleted the transmembrane region of TREM-1 in addition to the start site and first domain of TREM-3. The targeting construct was linearized and transfected into E14.1 (129P2/OlaHsd) ES cells. 450 clones were chosen and expanded in duplicate; genomic DNA isolated from one set was digested with KpnI (K) and hybridized with a 3′ external probe (B) on Southern blots (endogenous, 13.5 kb; targeted, 17.8 kb). One correctly targeted clone was identified and confirmed by Southern blot analysis using multiple digestions and 5′ (A), 3′ (B), and Neo probes. This clone was injected into C57BL/6 blastocysts; chimeras were bred to transgenic mice expressing Cre under the CMV promoter (59) on a C57BL/6 background to delete the MC1neopA gene (TREM-1/3 del). Transmission of the TREM-1/3 deletion in agouti offspring was determined by PCR using tail DNA as a template and the following oligonucleotides: TREM-1/3 28279, TCTTGCCGCTGATTGGTTCA; TREM-1/3 27096, TCCCAAGAGCAGGCACAAGA; TREM-1/3 19239, TCTCTCCATCTATGCATCCACCC; endogenous, 373 bp, deletion, 270 bp. Heterozygous mice were intercrossed to generate mice homozygous for the deletion.

*Speed congenics*. We backcrossed the TREM-1/3 mutation onto a C57BL/6 background facilitated by genome-wide simple sequence length polymorphism (SSLP) typing at 10-cm intervals for each generation (done by the Speed Congenics Facility supported by the Rheumatic Diseases Core Center at Washington University School of Medicine). The mice used for these experiments were >97% C57BL/6.

C57BL/6 mice were originally purchased from NCI. All animals used in this study were bred in a barrier facility at the University of Iowa. Mice used in pneumonia challenge studies were littermates or WT mice bred in our facility. The age of pneumonia experimental mice (55–75 days) was matched in WT and TREM-1/3–deficient mice. Mice used in all other experiments were <100 days of age.

*Pneumonia models*. *P. aeruginosa*, strain PA103, was grown overnight in LB broth and subcultured to mid-log phase and diluted to $2 \times 10^5$ CFU/ml. Mice were anesthetized with ketamine/xylazine, followed by intubation with a 24G catheter, and $1 \times 10^4$ CFU *P. aeruginosa* was instilled into the trachea. Mice recovered from anesthesia and were monitored for symptoms and temperature and euthanized when body temperature fell below 26°C or if they were moribund. Temperatures were determined using an Exergen Corp. Veterinary Infrared Tympanic Temperature Scanner, Model VTTS-1000. Survival studies were performed on separate animals. Mice in survival studies received no additional treatments.

*Plasma and tissue collection*. Pneumonia was induced as before in separate groups of mice. At 14 hours after infection, mice were anesthetized, and blood was collected in tubes containing 10 mM EDTA. Tubes were centrifuged at 1,000 *g* for 10 minutes at 4°C. Supernatant plasma was aspirated and stored in multiple aliquots at –80°C until analysis. For histology or organ cytokine assays, lungs and liver were perfused with PBS through a catheter placed in the right ventricle. An opening was made in the right atrium to allow fluids to escape. Mouse lungs were hand homogenized in a buffer containing 15 mM Tris, 0.5% Triton X-100, 150 mM NaCl, 1 mM $CaCl_2$, 1 mM $MgCl_2$, pH 7.4. Supernatants from homogenates were centrifuged at 1,000 *g* for 10 minutes at 4°C and stored in multiple aliquots at –80°C. Thawed lung homogenate supernatants were filtered through a 0.22-μm filter prior to analysis. For single-cell lung suspension analyses, perfused lungs were cut into small pieces and digested in 4 ml HBSS supplemented with 60 U/ml DNase I (Sigma-Aldrich) and 125 U/ml collagenase (Invitrogen) for 30 minutes at 37°C. Lung tissue was pressed through a wire mesh screen (Cellector, Bellco Glass) following digestion to create a single-cell suspension.

*Bone marrow–derived neutrophils*. Mice were euthanized, and bone marrow was collected from femurs and tibias. Cells were isolated on a discontinuous Percoll gradient (MB Biomedical) composed of 81%, 62%, 55%, and 50%, and cells between the 62% and 81% layers were collected. Red blood cells were lysed with RBC Lysis Buffer (eBioscience) and neutrophils suspended in HBSS, without $Ca^{2+}$ and $Mg^{2+}$, and held on ice prior to testing. Neutrophil preparations were routinely >70% pure as determined by Cytospin.

*Histology*. At 14 hours after infection with *P. aeruginosa*, mice were anesthetized and perfused with 20 ml PBS and 20 ml 4% formaldehyde, and then lungs were placed in vials containing 4% formaldehyde. Lungs were placed under vacuum overnight, paraffin embedded, and stained with H&E. Histologic analysis was performed by a veterinary pathologist unaware of sample identities. Bilateral lungs from 5 animals in each group were examined. The scoring system was as follows — for cellularity (most severe foci assessed in lung): 1, mild, scattered leukocytes in interstitium and airspaces; 2, moderate, scattered leukocytes forming aggregates in interstitium and perivascular spaces and extending into airspaces; 3, moderate to severe prominent leukocyte infiltration in interstitium extending

into airspaces often with prominent perivascular aggregates; for edema: 0, none; 1, mild, wispy eosinophilic material detectable in rare foci; 2, mild to moderate amounts of eosinophilic material detectable in scattered to coalescing foci; 3, moderate to extensive amounts of eosinophilic material filling alveoli. For necrotic foci, distinct necrotic cellular foci (often severely degenerated neutrophils with uncommon parenchymal components) in parenchyma were enumerated in the most severe region of each lung using ×200 magnification fields, 2 samples/slide × 2 slides (4 samples total).

*Lung scoring.* Right and left lungs were sectioned in the coronal plane. Using a stereotactic approach, grids were used to segment the parenchyma into squares, and random numbers were used to identify regions for analysis, except when anatomic-specific regions were assessed. All examination, morphometry, and scoring were done in manner blinded to treatment group. For bronchiole neutrophils, terminal bronchioles (TBs) were identified in sections of lung as small airways opening into alveolar ducts, and in each TB the number of neutrophils within the lumen and those in the submucosa (exterior to airway epithelium basement membrane) were enumerated. These were scored based on the relative proportion of neutrophils in each TB as follows: 1, interstitial neutrophils < luminal neutrophils; 0.5, interstitial neutrophils = luminal neutrophils; and 0, interstitial neutrophils > luminal neutrophils. For alveolar neutrophils, random sections of lung were assessed (×400 magnification, BX51 microscope, Olympus) for the number of neutrophils within alveoli, and these numbers were standardized as neutrophils per 100 alveoli (60).

*BAL.* At 14 hours after infection, mice were anesthetized, and the chest cavity was opened. The trachea was exposed, an incision made, and tubing inserted. The lungs were flushed with 3 × 1 ml PBS. Fluids were collected and volumes recorded. For bacterial counts, 100 μl fluid was removed and plated on LB agar as described below. The remaining fluid was centrifuged to remove cells, and supernatant was stored in aliquots at –80°C.

*Bacterial counts*. Bacterial load was determined by dilution and plate count on LB agar following standard microbiological methods. CFU were counted, and CFU/ml was calculated.

*Flow cytometry*. Heparinized whole blood was stained, and rbc were lysed with 150 mM $NH_4Cl$, 10 mM $KHCO_3$, 0.1 mM EDTA. BAL fluids were centrifuged and pelleted cells resuspended in 2% FBS in PBS for staining. BAL cells were incubated with mouse Fc Block (BD 553141) prior to additional staining. Blood and BAL were stained with anti-CD115 (eBioscience 12-1152) and anti-Ly6G (BD 551460), which is specific for Ly6G without Ly6C cross-reactivity, per the manufacturer's instructions. Cell type was determined by FACS on a BD LSR II with BD FACSDiva software. For single lung suspension analysis, a total of $2 \times 10^6$ lung cells were stained in a 96-well round-bottom plate. Lung homogenates were surface stained with mAbs specific to CD45, Ly6c, Ly6g, Siglec F (BD Biosciences), CD11c, F4/80, MHC II, CD4, CD8, B220, CD19, DX5, and CD3 for 30 minutes at 4°C and fixed with FACS lysing solution (BD Biosciences) for 10 minutes at room temperature. All monoclonal antibodies were purchased from BioLegend unless otherwise stated. Stained cells were run on a BD LSRFortessa. The total numbers of eosinophils ($CD11c^{int}$Siglec $F^+$), neutrophils ($Ly6c^+Ly6g^{hi}$), macrophages ($CD11c^+F4/80^+$), NK cells ($CD3^+DX5^+$), $CD4^+$ T cells ($CD3^+CD4^+$), $CD8^+$ T cells ($CD3^+CD8^+$), and B cells ($CD19^+B220^+$) were quantified using FlowJo (Tree Star) software.

*Cytokine and chemokine assays*. Plasma and BAL fluids were analyzed using the Milliplex Bead Assay (Millipore). Cytokines/chemokines were all quantified using a customized multiplex magnetic bead panel kit (catalog MCYTOMAG-70K, Millipore). The manufacturer's instructions were followed for assay parameters and protocol, with the following minor modification: 50 μl BAL fluid was used instead of the recommended 25 μl. G-CSF levels in mice subjected to bacterial challenge were extremely high compared with those of all other cytokines. Thus, G-CSF was not included in the multiplex panel but assayed independently at a 20-fold dilution using the same magnetic bead procedures. A Bio-Plex Pro II plate washer (Bio-Rad) was used to wash magnetic beads. Fluorescence intensity was measured on a Bio-Plex 200 system using Bio-Plex Manager software. Data collection parameters were set to 50 beads per region, 60-second timeout, bead map of 100 regions, sample size of 100 μl, and gate setting of 5,000–25,000.

*ALT serology*. ALT was determined from plasma collected as described above using Abaxis VetScan, Prep Profile II.

*Phagocytosis assay*. Murine bone marrow neutrophils were isolated as previously described and held on ice in HBSS, without $Ca^{2+}$ and $Mg^{2+}$. Texas red–zymosan particles (Molecular Probes, Invitrogen) were sonicated for 5 minutes, opsonized in normal mouse serum in the dark for 30 minutes at 37°C, washed, and resuspended at 0.4 M/ml in HBSS, with $Ca^{2+}$ and $Mg^{2+}$, 0.1% glucose, and 1% human serum albumin. 500,000 neutrophils were mixed with opsonized Texas red–zymosan at MOI of 1, 5, and 25 in 100 μl HBSS, with $Ca^{2+}$ and $Mg^{2+}$, 0.1% glucose, and 1% human serum albumin. The mixtures were incubated at 37°C for 30 minutes, then placed on wet ice for 5 minutes, stained with Ly6G-FITC (BD Biosciences — Pharmingen) for 20 minutes on ice, and washed. FACs was performed on a BD LSR II with BD FACSDiva software and analyzed using Cellquest software.

*Neutrophil bacterial killing.* Neutrophils were isolated from bone marrow as described and resuspended at $6 \times 10^5$/ml in HBSS without $Ca^{2+}$ and $Mg^{2+}$ and held on ice. An overnight culture of *P. aeruginosa* strain PA103 was subcultured until $OD_{600}$ was 0.6. One milliliter of culture was pelleted at 600 *g* for 5 minutes. The pellet was resuspended in 1 ml HBSS with $Ca^{2+}$ and $Mg^{2+}$, 0.5% BSA, and 10% pooled human serum and opsonized for 20 minutes at 37°C, with rotation. Bacteria were washed twice in ice-cold PBS and resuspended in 1 ml HBSS with $Ca^{2+}$ and $Mg^{2+}$ and 0.5% BSA. Bacteria were diluted to $2.5 \times 10^6$/ml in HBSS with $Ca^{2+}$ and $Mg^{2+}$ and 0.5% BSA. Neutrophils were mixed with bacteria at 1:1 for an MOI of 1:4 and incubated together at 37°C/5% $CO_2$, with rotation for 45 minutes. Gentamicin sulfate (Cellgro), 0.5 mg/ml, was added, and incubation continued for 15 minutes. The mixture was washed twice in PBS to remove gentamicin and free bacteria. Neutrophils were resuspended in HBSS with $Ca^{2+}$ and $Mg^{2+}$ and 0.5% BSA and returned to the incubator. Samples were taken at relevant time points, and neutrophils were washed once in ice-cold PBS and lysed with 100 μl LB broth plus 0.1% Triton X-100. Plate counts were made by serial dilution on LB agar.

*NADPH oxidase activity*. NADPH oxidase activity was determined using Fluostar Omega (BMG Technologies). Neutrophils were isolated from bone marrow of healthy mice as described and resuspended at $1 \times 10^6$ cells/ml in HBSS, with $Ca^{2+}$ and $Mg^{2+}$, 0.1% glucose, and 0.1% human serum albumin. 200 μl of cell suspension with lucigenin (Sigma-Aldrich) at a final concentration of 100 μM was stimulated with opsonized zymosan (OpZ) (Molecular Probes, Invitrogen) at a ratio of 2:1 OpZ to neutrophils or with 10 ng/ml PMA (Sigma-Aldrich). Zymosan particles were sonicated for 5 minutes, opsonized by incubation with pooled human serum for 30 minutes at 37°C, centrifuged, and resuspended in HBSS, with $Ca^{2+}$ and $Mg^{2+}$, 0.1% glucose, and 0.1% human serum albumin. Chemiluminescence readings were taken every minute for 60 minutes and reported as relative luminescence units per minute.

*Cell death assay*. $2 \times 10^5$ neutrophils resuspended in DMEM containing 10% FCS or not were cultured in tissue culture wells previously coated with BSA (100 ng/ml BSA in PBS, 2 hours at 37°C). Cell death was determined by the propidium iodide uptake assay of DNA content as previously described (25). In brief, cells were resuspended in 0.5 ml PBS and then fixed by adding 1.5 ml ice-cold 70% ethanol and incubating for 1 hour at 4°C. Fixed cells were washed once with 10 ml PBS containing 10% FCS, resuspended in the same buffer containing 40 μg/ml RNase A, and 50 μg/ml propidium iodide and incubated for 30 minutes in the dark. Samples were acquired by FACS, and cell death was determined based on hypodiploid DNA content.

*TX migration plate assay*. Murine bone marrow neutrophils were isolated as previously described and stained with calcein-AM (Invitrogen, C3099) at a final concentration of 5 μg/ml. Cells were incubated at 37°C for 30 minutes, washed, and stored in HBSS, without $Ca^{2+}$ and $Mg^{2+}$. Cells were diluted to $10^6$/ml in HBSS, with $Ca^{2+}$ and $Mg^{2+}$, 0.1% glucose, and 1% human serum albumin prior to addition to the plate. ZAS was prepared by incubating normal mouse serum with sonicated zymosan (Molecular Probes, Invitrogen) particles at 37°C for 30 minutes (61). The zymosan particles were removed by centrifugation, and the resulting serum was diluted to 10% in HBSS, with $Ca^{2+}$ and $Mg^{2+}$, 0.1% glucose, 1% human serum albumin. KC (R&D Systems, 1395-KC) was diluted to 50 nM and 5 nM in HBSS, with $Ca^{2+}$ and $Mg^{2+}$, 0.1% glucose, and 1% human serum albumin. DPBS without $Ca^{2+}$ and $Mg^{2+}$ was used to determine random migration. The TX migration plate (Neuroprobe, 101-3) consisted of a 3-μm pore filter in a 96-well format. 30 μl of stimulant or PBS was placed in the wells below the filter. The filter was snapped in place, and 25,000 neutrophils in 25 μl droplets were placed in hydrophobic rings on the filter, which allowed contact with the stimulant below. Additionally, a standard curve of stained cells was prepared from both cell preparations, and 25 μl placed in separate wells below the filter, with no fluid on the filter top. The prepared plate was incubated for 3 hours at 37°C/5% $CO_2$. Following incubation, the cells were removed from the top of the filter by gently wiping with tissues and rinsing with HBSS, without $Ca^{2+}$ and $Mg^{2+}$. The plate was read on a Tecan Safire2 at 485 nm (excitation) and 530 nm (emission). The number of migrated cells was calculated from the standard curves, based on relative fluorescence units, using Excel. Graphs were made using GraphPad Prism.

*Neutrophil migration across airway endothelial cells*. SVEC4-10 murine lymph node endothelial cells (ATCC CRL-2181) were grown in DMEM (Gibco, Invitrogen) supplemented with 10% FBS (Hyclone) and L-glutamine (Gibco). MBECs, a gift from Beverly Davidson (University of Iowa, Iowa City, Iowa, USA), were grown in DMEM/F12 (Gibco), supplemented with 10% FBS and 100 U/ml penicillin and 100 μg/ml streptomycin (Gibco). Endothelial cells were cultured on gelatin-coated, 3.0-μm-pore-size Transwell filters (Costar, 3472) for 3 days at 37°C/5% $CO_2$ with 1 ml of medium in the bottom chamber. Confluence was assessed by H&E staining. Freshly isolated neutrophils were diluted to $5 \times 10^6$/ml in HBSS, with $Ca2^+$ and $Mg2^+$, 0.1% glucose, and 1% human serum albumin. 100 μl of neutrophil suspension was added to the Transwell, and 1 ml of 10% ZAS/medium was placed in the chamber below. Neutrophils migrated in the apical-to-basolateral direction for 16 hours, and then were collected from the lower chamber and counted using a hemocytometer.

*Mouse endothelial cell isolation*. Murine pulmonary endothelial cells were isolated as previously described (26). Mice were anesthetized with ketamine/xylazine. The lungs were perfused with 10 ml of 2-mM EDTA in PBS, followed by 5 ml 0.25% trypsin/2 mM EDTA via the right ventricle. The lungs were removed and incubated at 37°C for 30 minutes in PBS. The lungs were minced with a sterile blade, suspended in 2 ml DMEM plus 10% FBS, and washed 10 times to elute cells from the lung. Cells, but not debris, were placed in a 15-ml conical tube and centrifuged 5 minutes at 250 *g*. Cells were resuspended in 1.5 ml EGB-2 medium, 2% FBS, and supplements (EGM-2 Bullet Kit, Lonza CC3162) and plated in two 6-well plates precoated with 0.2% gelatin/PBS. Medium was changed at 24 hours and every other day until use.

*Neutrophil migration across AECs*. Mouse tracheal AECs were cultured on 3-μm-pore-size Transwell filter (Costar, 3470) based on a previous report (27). Two weeks after seeding, the differentiated AECs established transepithelial resistance >500 Ω•$cm^2$. To investigate the transepithelial migration ability of neutrophils, freshly isolated bone marrow derived neutrophils pooled from 3 mice per group (200,000/well) were loaded on the basolateral side of AECs by inverting the Transwells. KC (50 nM) was added at the apical side of culture medium. After 16 hours of co-incubation, the cells in apical medium were collected and cytospinned on a glass microscope slide. Ly6G immunostaining was performed to identify neutrophils. $Ly6G^+$ cells were quantified by counting 3 random fields under a ×20 objective lens.

*TEM*. Filters for TEM were processed using conventional methods. Briefly, samples were fixed in 2.5% gluteraldehyde in 0.1 M cacodylate buffer, postfixed in 1% osmium tetroxide, and en bloc stained in 2.5% aqueous uranyl acetate. The filters were then dehydrated in a graded series of ethanol washes, transitioned to Eponate-12 resin (Ted Pella Inc.), and cured overnight at 65°C. Ultrathin sections were post-stained with uranyl acetate and lead citrate and imaged in a JEOL JEM 1230 transmission electron microscope equipped with a Gatan 2k × 2k digital camera.

*Statistics*. Unless otherwise noted, all data were evaluated using GraphPad Prism software. Error bars represent SEM. Statistical significance was determined by Mann-Whitney nonparametric *t* test. For cytokine assays, geometric mean fluorescence (MF) was analyzed using a 5-parameter logistic equation. Based on expected/observed concentration ratios, interpolated values greater than 10,000 pg/ml (highest concentration used for standard curve) were all arbitrarily set to 12,000 pg/ml, while values calculated to be less than 16 pg/ml were all set to 0. In the case of G-CSF, the upper limit was set to 240 ng/ml and the lower limit to 300 pg/ml. A statistical software package (SAS) was used to assess differences in concentrations of each cytokine between WT (C57BL/6) mice and TREM-1/3–deficient mice using the nonparametric Wilcoxon test. *P* values less than 0.05 were considered significant. For single lung suspension analysis, statistical analyses were performed using InStat software (GraphPad Software). Groups were compared using 2-way ANOVA with Bonferroni post-test analyses to determine whether there was a statistical significance of at least $\alpha = 0.05$.

*Study approval*. All protocols involving mice were approved by the University of Iowa Institutional Animal Care and Use Committee and were carried out in accordance with institutional guidelines and regulations. TREM-1/3–deficient animals were generated at Washington University in St. Louis with the approval of the Washington University Animal Care and Use Committee and were carried out in accordance with institutional guidelines and regulations.

## Acknowledgments

We thank Bill Nauseef, Beverly Davidson, and Kristina Thiel for critical reading and editing of the manuscript. We also thank Mark Schultz for assistance with the MBECs. This work was supported by grants from the American Heart Association to J. Klesney-Tait (0675028N) and from the NIH to M. Colonna (GM077279-04). All imaging was carried out by the Central Microscopy Research Facilities. The data presented herein were obtained at the Flow Cytometry Facility, which is a Carver College of Medicine Core Research Facilities/Holden Comprehensive Cancer Center Core Laboratory at the University of Iowa. The Facility is funded through user fees and the financial support of the Carver College of Medicine, Holden Comprehensive Cancer Center, and Iowa City Veteran's Administration Medical Center.

Received for publication April 13, 2012, and accepted in revised form October 11, 2012.

Address correspondence to: Julia Klesney-Tait, Department of Internal Medicine, Roy J. and Lucille A. Carver College of Medicine, University of Iowa, 200 Hawkins Dr., Iowa City, Iowa 52242, USA. Phone: 319.356.3576; Fax: 319.353.6406; E-mail: julia-klesney-tait@uiowa.edu.

1. Borregaard N. Neutrophils, from marrow to microbes. *Immunity*. 2010;33(5):657–670.
2. Mantovani A, Cassatella MA, Costantini C, Jaillon S. Neutrophils in the activation and regulation of innate and adaptive immunity. *Nat Rev Immunol*. 2011;11(8):519–531.
3. Beutler B. Inferences, questions and possibilities in Toll-like receptor signaling. *Nature*. 2004; 430(6996):257–263.
4. Klesney-Tait J, Turnbull IR, Colonna M. The TREM receptor family and signal integration. *Nat Immunol*. 2006;7(12):1266–1273.
5. Kawai T, Akira S. Toll-like receptors and their crosstalk with other innate receptors in infection and immunity. *Immunity*. 2011;34(5):637–650.
6. Agarwal PK, Kumari R. Sepsis--theory and therapies. *N Engl J Med*. 2003;348(16):1600–1602.
7. Bouchon A, Dietrich J, Colonna M. Cutting edge: inflammatory responses can be triggered by TREM-1, a novel receptor expressed on neutrophils and monocytes. *J Immunol*. 2000;164(10):4991–4995.
8. Gibot S. Soluble triggering receptor expressed on myeloid cells and the diagnosis of pneumonia. *N Engl J Med*. 2004;350(5):451–458.
9. Gibot S. Plasma level of a triggering receptor expressed on myeloid cells-1: its diagnostic accuracy in patients with suspected sepsis. *Ann Intern Med*. 2004;141(1):9–15.
10. Bouchon A, Facchetti F, Weigand MA, Colonna M. TREM-1 amplifies inflammation and is a crucial mediator of septic shock. *Nature*. 2001; 410(6832):1103–1107.
11. Nathan C, Ding A. TREM-1: a new regulator of innate immunity in sepsis syndrome. *Nat Med*. 2001; 7(5):530–532.
12. Bleharski JR. A role for triggering receptor expressed on myeloid cells-1 in host defense during the early-induced and adaptive phases of the immune response. *J Immunol*. 2003;170(7):3812–3818.
13. Ornatowska M, et al. Functional genomics of silencing TREM-1 on TLR4 signaling in macrophages. *Am J Physiol Lung Cell Mol Physiol*. 2007; 293(6):L1377–L1384.
14. Nathan C. Neutrophils and immunity: challenges and opportunities. *Nat Rev Immunol*. 2006; 6(3):173–182.
15. Hotchkiss RS, Karl IE. The pathophysiology and treatment of sepsis. *N Engl J Med*. 2003;348(2):138–150.
16. Ramphal R, Balloy V, Huerre M, Si-Tahar M, Chignard M. TLRs 2 and 4 are not involved in hypersusceptibility to acute pseudomonas aeruginosa lung infections. *J Immunol*. 2005;175(6):3927–3934.
17. Gibot S, et al. Modulation of the triggering receptor expressed on myeloid cells–1 pathway during pneumonia in rats. *J Infect Dis*. 2006;194(7):975–983.
18. Gibot S, et al. A soluble form of the triggering receptor expressed on myeloid cells-1 modulates the inflammatory response in murine sepsis. *J Exp Med*. 2004;200(11):1419–1426.
19. Gibot S, et al. TREM-1 promotes survival during septic shock in mice. *Eur J Immunol*. 2007; 37(2):456–466.
20. Chung DH, Seaman WE, Daws MR. Characterization of TREM-3, an activating receptor on mouse macrophages: definition of a family of single Ig domain receptors on mouse chromosome 17. *Eur J Immunol*. 2002;32(1):59–66.
21. Hed J, Hallden G, Johansson SGO, Larsson P. The use of fluorescence quenching in flow cytofluorometry to measure the attachment and ingestion phases in phagocytosis in peripheral blood without prior cell separation. *J Immunol Methods*. 1987;101(1):119–125.
22. Moreland JG, et al. Endotoxin priming of neutrophils requires NADPH oxidase-generated oxidants and is regulated by the anion transporter ClC-3. *J Biol Chem*. 2007;282(47):33958–33967.
23. Van Ziffle JA, Lowell CA. Neutrophil-specific deletion of Syk kinase results in reduced host defense to bacterial infection. *Blood*. 2009;114(23):4871–4882.
24. Weiss J, Victor M, Stendhal O, Elsbach P. Killing of gram-negative bacteria by polymorphonuclear leukocytes: role of an O2-independent bactericidal system. *J Clin Invest*. 1982;69(4):959–970.
25. Otero K, et al. Macrophage colony-stimulating factor induces the proliferation and survival of macrophages via a pathway involving DAP12 and [beta]-catenin. *Nat Immunol*. 2009;10(7):734–743.
26. Chen X, et al. Increased plasma MMP9 in integrin alpha1-null mice enhances lung metastasis of colon carcinoma cells. *Int J Cancer*. 2005;116(1):52–61.
27. You Y, Richer EJ, Huang T, Brody SL. Growth and differentiation of mouse tracheal epithelial cells: selection of a proliferative population. *Am J Physiol Lung Cell Mol Physiol*. 2002;283(6):L1315–L1321.
28. Williams BG, Gouws E, Boschi-Pinto C, Bryce J, Dye C. Estimates of world-wide distribution of child deaths from acute respiratory infections. *Lancet Infect Dis*. 2002;2(1):25–32.
29. Kreisel D, et al. In vivo two-photon imaging reveals monocyte-dependent neutrophil extravasation during pulmonary inflammation. *Proc Natl Acad Sci U S A*. 2010;107(42):18073–18078.
30. Woodfin A, et al. The junctional adhesion molecule JAM-C regulates polarized transendothelial migration of neutrophils in vivo. *Nat Immunol*. 2011; 12(8):761–769.
31. Nourshargh S, Hordijk PL, Sixt M. Breaching multiple barriers: leukocyte motility through venular walls and the interstitium. *Nat Rev Mol Cell Biol*. 2010;11(5):366–378.
32. Wagner JG, Roth RA. Neutrophil migration mechanisms, with an emphasis on the pulmonary vasculature. *Pharmacol Rev*. 2000;52(3):349–374.
33. Spertini O, et al. Leukocyte adhesion molecule-1 (LAM-1, L-selectin) interacts with an inducible endothelial cell ligand to support leukocyte adhesion. *J Immunol*. 1991;147(8):2565–2573.
34. von Andrian UH, Chambers JD, McEvoy LM, Bargatze RF, Arfors KE, Butcher EC. Two-step model of leukocyte-endothelial cell interaction in inflammation: distinct roles for LECAM-1 and the leukocyte beta 2 integrins in vivo. *Proc Natl Acad Sci U S A*. 1991;88(17):7538–7542.
35. Muller WA. Mechanisms of leukocyte transendothelial migration. *Annu Rev Pathol*. 2011;6:323–344.
36. Doerschuk CM, Allard MF, Martin BA, MacKenzie A, Autor AP, Hogg JC. Marginated pool of neutrophils in rabbit lungs. *J Appl Physiol*. 1987; 63(5):1806–1815.
37. Doerschuk CM, Beyers N, Coxson HO, Wiggs B, Hogg JC. Comparison of neutrophil and capillary diameters and their relation to neutrophil sequestration in the lung. *J Appl Physiol*. 1993;74(6):3040–3045.
38. Gee MH, Albertine KH. Neutrophil-endothelial cell interactions in the lung. *Annu Rev Physiol*. 1993; 55:227–248.
39. Gebb SA, et al. Sites of leukocyte sequestration in the pulmonary microcirculation. *J Appl Physiol*. 1995; 79(2):493–497.
40. Diamond MS, Springer TA. A subpopulation of Mac-1 (CD11b/CD18) molecules mediates neutrophil adhesion to ICAM-1 and fibrinogen. *J Cell Biol*. 1993;120(2):545–556.
41. Lehmann JCU, Jablonski-Westrich D, Haubold U, Gutierrez-Ramos J-C, Springer T, Hamann A. Overlapping and selective roles of endothelial intercellular adhesion molecule-1 (ICAM-1) and ICAM-2 in lymphocyte trafficking. *J Immunol*. 2003; 171(5):2588–2593.
42. Morland CM, Morland BJ, Darbyshire PJ, Stockley RA. Migration of CD18-deficient neutrophils in vitro: evidence for a CD18-independent pathway induced by IL-8. *Biochim Biophys Acta*. 2000; 1500(1):70–76.
43. O'Brien CD, Lim P, Sun J, Albelda SM. PECAM-1–dependent neutrophil transmigration is independent of monolayer PECAM-1 signaling or localization. *Blood*. 2003;101(7):2816–2825.
44. Muller WA, Weigl SA, Deng X, Phillips DM. PECAM-1 is required for transendothelial migration of leukocytes. *J Exp Med*. 1993;178(2):449–460.
45. Vaporciyan AA, et al. Involvement of platelet-endothelial cell adhesion molecule-1 in neutrophil recruitment in vivo. *Science*. 1993;262(5139):1580–1582.
46. Sachs UJ, et al. The neutrophil-specific antigen CD177 is a counter-receptor for platelet endothelial cell adhesion molecule-1 (CD31). *J Biol Chem*. 2007;282(32):23603–23612.
47. Liu Y, et al. Signal regulatory protein (SIRPalpha), a cellular ligand for CD47, regulates neutrophil transmigration. *J Biol Chem*. 2002;277(12):10028–10036.
48. McDonald RJ, St George JA, Pan LC, Hyde DM. Neutrophil adherence to airway epithelium is reduced by antibodies to the leukocyte CD11/CD18 complex. *Inflammation*. 1993;17(2):145–151.
49. Celi A, Cianchetti S, Petruzzelli S, Carnevali S, Baliva F, Giuntini C. ICAM-1-independent adhesion of neutrophils to phorbol ester-stimulated human airway epithelial cells. *Am J Physiol*. 1999; 277(3 pt 1):L465–L471.
50. Jagels MA, Daffern PJ, Zuraw BL, Hugli TE. Mechanisms and regulation of polymorphonuclear leukocyte and eosinophil adherence to human airway epithelial cells. *Am J Respir Cell Mol Biol*. 1999; 21(3):418–427.
51. Tosi MF, Hamedani A, Brosovich J, Alpert SE. ICAM-1-independent, CD18-dependent adhesion between neutrophils and human airway epithelial cells exposed in vitro to ozone. *J Immunol*. 1994; 152(4):1935–1942.
52. Tosi MF, Stark JM, Smith CW, Hamedani A, Gruenert DC, Infeld MD. Induction of ICAM-1 expression on human airway epithelial cells by inflammatory cytokines: effects on neutrophil-epithelial cell adhesion. *Am J Respir Cell Mol Biol*. 1992;7(2):214–221.
53. Burns AR, Takei F, Doerschuk CM. Quantitation of ICAM-1 expression in mouse lung during pneumonia. *J Immunol*. 1994;153(7):3189–3198.
54. Kang BH, Crapo JD, Wegner CD, Letts LG, Chang LY. Intercellular adhesion molecule-1 expression on the alveolar epithelium and its modification by hyperoxia. *Am J Respir Cell Mol Biol*. 1993;9(4):350–355.
55. Taguchi M, et al. Patterns for RANTES secretion and intercellular adhesion molecule 1 expression mediate transepithelial T cell traffic based on analyses in vitro and in vivo. *J Exp Med*. 1998; 187(12):1927–1940.
56. Zen K, Babbin BA, Liu Y, Whelan JB, Nusrat A, Parkos CA. JAM-C is a component of desmosomes and a ligand for CD11b/CD18-mediated neutrophil transepithelial migration. *Mol Biol Cell*. 2004; 15(8):3926–3937.
57. Zen K, et al. Neutrophil migration across tight junctions is mediated by adhesive interactions between epithelial coxsackie and adenovirus receptor and a junctional adhesion molecule-like protein on neutrophils. *Mol Biol Cell*. 2005;16(6):2694–2703.
58. Parkos CA, et al. CD47 mediates post-adhesive events required for neutrophil migration across polarized intestinal epithelia. *J Cell Biol*. 1996; 132(3):437–450.
59. Schwenk F, Baron U, Rajewsky K. A cre-transgenic mouse strain for the ubiquitous deletion of loxP-flanked gene segments including deletion in germ cells. *Nucleic Acids Res*. 1995;23(24):5080–5081.
60. Bullard DC, et al. P-selectin/ICAM-1 double mutant mice: acute emigration of neutrophils into the peritoneum is completely absent but is normal into pulmonary alveoli. *J Clin Invest*. 1995; 95(4):1782–1788.
61. Biesecker G, Wagner J, Hugli T. The release of C5a in complement-activated serum does not require C6. *J Immunol*. 1989;143(4):1228–1232.